NASA Tech Briefs

NATIONAL AERONAUTICS AND SPACE ADMINISTRATION

INTRODUCTION

Tech Briefs are short announcements of innovations originating from research and development activities of the National Aeronautics and Space Administration. They emphasize information considered likely to be transferable across industrial, regional, or disciplinary lines and are issued to encourage commercial application.

Additional Information on NASA Tech Briefs and TSPs

Additional information announced herein may be obtained from the NASA Technical Reports Server: **http://ntrs.nasa.gov**.

Please reference the control numbers appearing at the end of each Tech Brief. Information on NASA's Innovative Partnerships Program (IPP), its documents, and services is available on the World Wide Web at **http://www.ipp.nasa.gov**.

Innovative Partnerships Offices are located at NASA field centers to provide technology-transfer access to industrial users. Inquiries can be made by contacting NASA field centers listed below.

NASA Field Centers and Program Offices

Ames Research Center
David Morse
(650) 604-4724
david.r.morse@nasa.gov

Dryden Flight Research Center
Ron Young
(661) 276-3741
ronald.m.young@nasa.gov

Glenn Research Center
Kimberly A. Dalgleish-Miller
(216) 433-8047
kimberly.a.dalgleish@nasa.gov

Goddard Space Flight Center
Nona Cheeks
(301) 286-5810
nona.k.cheeks@nasa.gov

Jet Propulsion Laboratory
Indrani Graczyk
(818) 354-2241
indrani.graczyk@jpl.nasa.gov

Johnson Space Center
John E. James
(281) 483-3809
john.e.james@nasa.gov

Kennedy Space Center
David R. Makufka
(321) 867-6227
david.r.makufka@nasa.gov

Langley Research Center
Michelle Ferebee
(757) 864-5617
michelle.t.ferebee@nasa.gov

Marshall Space Flight Center
Terry L. Taylor
(256) 544-5916
terry.taylor@nasa.gov

Stennis Space Center
Ramona Travis
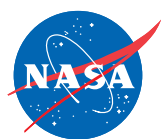(228) 688-3832
ramona.e.travis@ssc.nasa.gov

NASA Headquarters

Daniel Lockney,
Technology Transfer Program Executive
(202) 358-2037
daniel.p.lockney@nasa.gov

Small Business Innovation Research (SBIR) & Small Business Technology Transfer (STTR) Programs
Rich Leshner, Program Executive
(202) 358-4920
rleshner@nasa.gov

TECH BRIEFS

NATIONAL AERONAUTICS AND SPACE ADMINISTRATION

An "Inefficient Fin" Non-Dimensional Parameter to Measure Gas Temperatures Efficiently

This method provides a convenient sensing error guideline.

Dryden Flight Research Center, Edwards, California

A gas containment vessel that is not in thermal equilibrium with the bulk gas can affect its temperature measurement. The physical nature of many gas dynamics experiments often makes the accurate measurement of temperature a challenge. The environment itself typically requires that the thermocouple be sheathed, both to protect the wires and hot junction of the instrument from their environment, and to provide a smooth, rigid surface for pressure sealing of the enclosure. However, that enclosure may also be much colder than the gas to be sensed, or vice-versa. Either way, the effect of such gradients is to potentially skew the temperature measurements themselves, since heat may then be conducted by the instrument.

Thermocouple designers traditionally address this problem by insulating the sheath from the thermocouple leads and hot junction as much as possible. The thermocouple leads are typically packed in a ceramic powder inside the sheath, protecting them somewhat from temperature gradients along the sheath, but there is no effective mechanism to shield the sheath from the enclosure body itself. Standard practice dictates that thermocouples be used in installations that do not present large thermal gradients along the probe. If this conduction dominates heat transfer near the tip of the probe, then temperature measurements may be expected to be skewed. While the same problem may be experienced in the measurement of temperature at various points within a solid in a gradient, it tends to be aggravated in the measurements of gas temperature, since heat transfer dependent on convection is often less efficient than conduction along the thermocouple.

The proposed solution is an inefficient fin thermocouple probe. Conventional wisdom suggests that in many experiments where gas flows through an enclosure (e.g., flow in pipe, manifold,
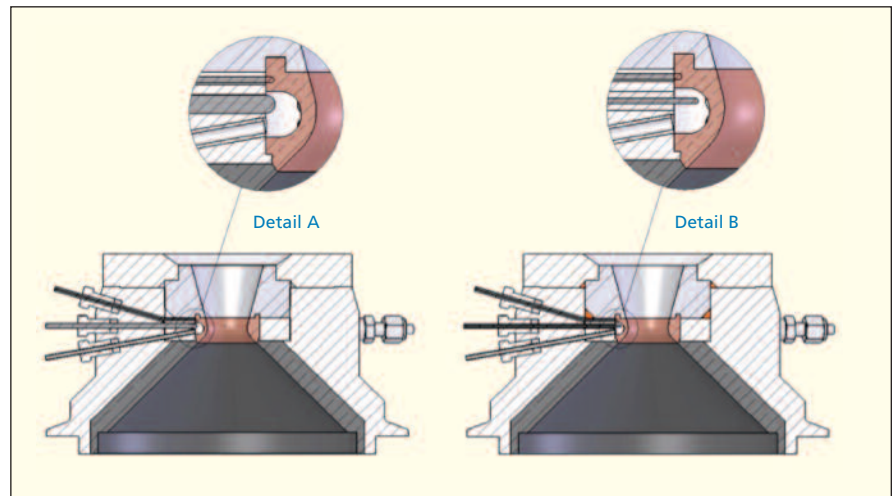
A **Schematic of the Apparatus Used in the Rocket Throat Cooling Experiment**. The three instruments measure throat temperature, gas temperature, and gas pressure (top to bottom). At left, the gas-sensing probe is nearly flush with the inner surface of the throat, corresponding with a low inefficient fin non-dimensional number. At right, the *D* (probe diameter) and *L* (distance past the enclosure wall) were changed to correspond to a non-dimensional number of 4.60.

nozzle, etc.), the thermocouple be introduced flush to the surface, so as not to interfere with the flow. In practice, however, many such experiments take place where the flow is already turbulent, so that a protruding thermocouple probe has a negligible effect on the flow characteristics. The key question then becomes just how far into the flow should a thermocouple protrude in order to properly sense the gas temperature at that point. Modeling the thermocouple as an "inefficient fin" directly addresses this question. The appropriate assumptions in this case are: one-dimensional conduction along the fin; steady-state, constant, and homogeneous thermal conductivity; negligible radiation; and a uniform, constant heat transfer coefficient over the probe surface. It is noted that the nature of the ceramic-filled probe makes the key assumption of homogeneous thermal conductivity that much more conservative.

Normally a mathematical expression is used to assess fin efficiency, i.e., how far from the fin base heat can be carried. In this case, however, the thermocouple probe should be designed to be an inefficient fin; that is, parameters should be chosen such that the temperature of the wall does not affect the temperature sensed at the tip of the probe. This inefficient fin parameter is then numerically equal to $\ln(l00/\%\ error)$, where % error is computed with respect to the temperature difference between the wall and the fluid. A one-to-one correspondence between this parameter and the error in sensed temperature may thus be established. For example, for a maximum error of 5%, the non-dimensional parameter value is 3.00. For an error of 1%, the target parameter value becomes 4.60. This parameter dictates the minimum distance for a given probe.

This simple method provides a convenient guideline to maintain flow temperature sensing error within a predefined range, given a temperature mismatch between a gas and its surrounding walls. This approach was put

to practice in such an experiment, where a hot rocket nozzle was cooled using a two-phase fluid (where the fluid temperature may thus be verified, using the saturation pressure). The measured temperature in the cooling annulus showed good agreement with the method, and the thermocouple became essentially insulated from the wall by setting the hot junction at a distance corresponding to the parameter value of 4.60.

On-Wafer Measurement of a Multi-Stage MMIC Amplifier With 10 dB of Gain at 475 GHz

Imaging applications include hidden weapons detection, troop protection, and airport security.

NASA's Jet Propulsion Laboratory, Pasadena, California

JPL has measured and calibrated a WR2.2 waveguide wafer probe from GGB Industries in order to allow for measurement of circuits in the 325–500 GHz range. Circuits were measured, and one of the circuits exhibited 10 dB of gain at 475 GHz.

The MMIC circuit was fabricated at Northrop Grumman Corp. (NGC) as part of a NASA Innovative Partnerships Program, using NGC's 35-nm-gate-length InP HEMT process technology. The chip utilizes three stages of HEMT amplifiers, each having two gate fingers of 10 μm in width. The circuits use grounded coplanar waveguide topology on a 50-μm-thick substrate with through substrate vias. Broadband matching is achieved with coplanar waveguide trans-

mission lines, on-chip capacitors, and open stubs. When tested with wafer probing, the chip exhibited 10 dB of gain at 475 GHz, with over 9 dB of gain from 445–490 GHz.

Low-noise amplifiers in the 400–500 GHz range are useful for astrophysics receivers and earth science remote sensing instruments. In particular, molecular lines in the 400–500 GHz range include the CO 4-3 line at 460 GHz, and the CI fine structure line at 492 GHz. Future astrophysics heterodyne instruments could make use of high-gain, low-noise amplifiers such as the one described here. In addition, earth science remote sensing instruments could also make use of low-noise receivers with MMIC amplifier front ends.

Present receiver technology typically employs mixers for frequency down-conversion in the 400–500 GHz band. Commercially available mixers have typical conversion loss in the range of 7–10 dB with noise figure of 1,000 K. A low-noise amplifier placed in front of such a mixer would have 10 dB of gain and lower noise figure, particularly if cooled to low temperature. Future work will involve measuring the noise figure of this amplifier.

Software to Control and Monitor Gas Streams

John F. Kennedy Space Center, Florida

This software package interfaces with various gas stream devices such as pressure transducers, flow meters, flow controllers, valves, and analyzers such as a mass spectrometer. The software provides excellent user interfacing with various windows that provide time-domain graphs, valve state buttons, priority-colored messages, and warning icons. The user can configure the software to save as much or as little data as needed to a comma-delimited file. The software also includes an intuitive scripting language for automated processing. The configuration allows for the assignment of measured values or calibration so that raw signals can be viewed as usable pressures, flows, or concentrations in real time. The software is based on those used in two safety systems for shuttle processing

and one volcanic gas analysis system.

Mass analyzers typically have very unique applications and vary from job to job. As such, software available on the market is usually inadequate or targeted on a specific application (such as EPA methods). The goal was to develop powerful software that could be used with prototype systems. The key problem was to generalize the software to be easily and quickly reconfigurable.

At Kennedy Space Center (KSC), the prior art consists of two primary methods. The first method was to utilize LabVIEW and a commercial data acquisition system. This method required rewriting code for each different application and only provided raw data. To obtain data in engineering units, manual calculations were required. The second method was to utilize one of the

embedded computer systems developed for another system. This second method had the benefit of providing data in engineering units, but was limited in the number of control parameters.

Other products allow the same end effect, except multiple computers would be required along with multiple software packages. This is compounded by the difficulty in timing the various software products. The software package described here is a combination of gas stream monitoring software products. It combines pressure monitoring and control, fluid flow monitoring and control, and many chemical analysis products, including, but not limited to, mass analyzers, turbo pumps, dew point sensors, oxygen sensors, temperature sensors, and the like. It allows for real-time display of raw data as well as reassigned cal-

ibration data. The software is capable of timing events as well as running scripts for semi-autonomous operation. The software also records this variety of data with proper timing.

This complex software package is composed of two primary parts: hardware communications and user interfacing. The hardware interfacing section allows for the computer to transfer data and commands (via digital or analog signals) to a wide variety of system components such as sensors, valves, transducers, analyzers, pumps, etc. The hardware interfacing section also allows for the recording of the transferred data/commands to be stored on the local computer. The user interface section gathers the data from the hardware interfacing section and presents it to the user in various user-configurable methods. The two most common methods of providing data to the user are via time-domain charting and real-time parameter value/status.

Miniaturized Laser Heterodyne Radiometer (LHR) for Measurements of Greenhouse Gases in the Atmospheric Column

Instrument could be used to validate other Earth observing missions.

Goddard Space Flight Center, Greenbelt, Maryland

This passive laser heterodyne radiometer (LHR) instrument simultaneously measures multiple trace gases in the atmospheric column including carbon dioxide (CO_2) and methane (CH_4), and resolves their concentrations at different altitudes. This instrument has been designed to operate in tandem with the passive aerosol sensor currently used in AERONET (an established network of more than 450 ground aerosol monitoring instruments worldwide). Because aerosols induce a radiative effect that influences terrestrial carbon exchange, simultaneous detection of aerosols with these key carbon cycle gases offers a uniquely comprehensive measurement approach.

Laser heterodyne radiometry is a technique for detecting weak signals that was adapted from radio receiver technology. In a radio receiver, a weak input signal from a radio antenna is mixed with a stronger local oscillator signal. The mixed signal (beat note, or intermediate frequency) has a frequency equal to the difference between the input signal and the local oscillator. The intermediate frequency is amplified and sent to a detector that extracts the audio from the signal.

In the LHR instrument described here, sunlight that has undergone absorption by the trace gas is mixed with laser light at a frequency matched to a trace gas absorption feature in the infrared (IR). Mixing results in a beat signal in the RF (radio frequency) region that can be related to the atmospheric concentration. For a one-second integration, the estimated column sensitivities are 0.1 ppmv for CO_2, and <1 ppbv for CH_4.

In addition to producing a standalone ground measurement product, this instrument could be used to calibrate/validate four Earth observing missions: ASCENDS (Active Sensing of CO_2 Emissions over Nights, Days, and Seasons), OCO-2 (Orbiting Carbon Observatory), OCO-3, and GOSAT (Greenhouse gases Observational SATellite).

The only network that currently measures CO_2 and CH_4 in the atmospheric column is TCCON (Total Carbon Column Observing Network), and only two of its 16 operational sites are in the United States. TCCON data is used for validation of GOSAT data, and will be used for OCO-2 validation. While these Fourier-transform spectrometers (FTS) can measure the largest range of trace gases, the network is severely limited due to the high cost and extreme size of these instruments (these occupy small buildings and require personnel for operation). The LHR/AERONET instrument offers a significantly smaller (carry-on luggage size) autonomous instrument that can be incorporated into AERONET's much larger (450 instruments) global network.

Anomaly Detection in Test Equipment via Sliding Mode Observers

Commercial applications of the algorithms exist in the oil, natural gas, and chemical industries for identifying and localizing leaks.

Stennis Space Center, Mississippi

Nonlinear observers were originally developed based on the ideas of variable structure control, and for the purpose of detecting disturbances in complex systems. In this anomaly detection application, these observers were designed for estimating the distributed state of fluid flow in a pipe described by a class of advection equations.

The observer algorithm uses collected data in a piping system to estimate the distributed system state (pressure and velocity along a pipe containing liquid gas propellant flow) using only boundary measurements. These estimates are then used to further estimate and localize possible anomalies such as leaks or foreign objects, and instrumentation metering problems such as incorrect flow meter orifice plate size.

The observer algorithm has the following parts: a mathematical model of the fluid flow, observer control algorithm, and an anomaly identification algorithm. The main functional opera-

tion of the algorithm is in creating the sliding mode in the observer system implemented as software. Once the sliding mode starts in the system, the equivalent value of the discontinuous function in sliding mode can be obtained by filtering out the high-frequency chattering component. In control theory, "observers" are dynamic algorithms for the online estimation of the current state of a dynamic system by measurements of an output of the system. Classical linear observers can provide optimal estimates of a system state in case of uncertainty modeled by white noise. For nonlinear cases, the theory of nonlinear observers has been developed and its success is mainly due to the sliding mode approach.

Using the mathematical theory of variable structure systems with sliding modes, the observer algorithm is designed in such a way that it steers the output of the model to the output of the system obtained via a variety of sensors, in spite of possible mismatches between the assumed model and actual system. The unique properties of sliding mode control allow not only control of the model internal states to the states of the real-life system, but also identification of the disturbance or anomaly that may occur.

Absolute Position of Targets Measured Through a Chamber Window Using Lidar Metrology Systems

This technique can be used to measure objects in thermal-vacuum chamber test environments, in furnaces used to forge items for manufacturing, and for measuring chemically volatile or radioactive materials through a window.

Goddard Space Flight Center, Greenbelt, Maryland

Lidar is a useful tool for taking metrology measurements without the need for physical contact with the parts under test. Lidar instruments are aimed at a target using azimuth and elevation stages, then focus a beam of coherent, frequency modulated laser energy onto the target, such as the surface of a mechanical structure. Energy from the reflected beam is mixed with an optical reference signal that travels in a fiber path internal to the instrument, and the range to the target is calculated based on the difference in the frequency of the returned and reference signals. In cases when the parts are in extreme environments, additional steps need to be taken to separate the operator and lidar from that environment. A model has been developed that accurately reduces the lidar data to an absolute position and accounts for the three media in the testbed — air, fused silica, and vacuum — but the approach can be adapted for any environment or material.

The accuracy of laser metrology measurements depends upon knowing the parameters of the media through which the measurement beam travels. Under normal conditions, this means knowledge of the temperature, pressure, and humidity of the air in the measurement volume. In the past, chamber windows have been used to separate the measuring device from the extreme environment within the chamber and still permit optical measurement, but, so far, only relative changes have been diagnosed. The ability to make accurate measurements through a window presents a challenge as there are a number of factors to consider.

In the case of the lidar, the window will increase the time-of-flight of the laser beam causing a ranging error, and refract the direction of the beam causing angular positioning errors. In addition, differences in pressure, temperature, and humidity on each side of the window will cause slight atmospheric index changes and induce deformation and a refractive index gradient within the window. Also, since the window is a dispersive media, the effect of both phase and group indices have to be considered. Taking all these factors into account, a method was developed to measure targets through multiple regions of different materials and produce results that are absolute measurements of target position in three-dimensional space, rather than simply relative position.

The environment in which the lidar measurements are taken must be broken down into separate regions of interest and each region solved for separately. In this case, there were three regions of interest: air, fused silica, and vacuum. The angular position of the target inside the chamber is solved using only phase index and phase velocity, while the ranging effects due to travel from air to glass to vacuum/air are solved with group index and group velocity. When all parameters are solved simultaneously, an absolute knowledge of the position of each target within an environmental chamber can be derived.

Novel features of this innovation include measuring absolute position of targets through multiple dispersive and non-dispersive media, deconstruction of lidar raw data from a commercial off-the-shelf unit into reworkable parameters, and use of group velocities to reduce range data. Measurement of structures within a vacuum chamber or other harsh environment, such as a furnace, may now be measured as easily as if they were in an ambient laboratory. This analysis permits transformation of the raw data into absolute spatial units (e.g., mm).

This technique has also been extended to laser tracker, theodolite, and cathetometer measurements through refractive media.

Goldstone Solar System Radar Waveform Generator

Pre-distortion of the transmitted signal to compensate for time-base distortion allows reception of an undistorted signal.

NASA's Jet Propulsion Laboratory, Pasadena, California

Due to distances and relative motions among the transmitter, target object, and receiver, the time-base between any transmitted and received signal will undergo distortion. Pre-distortion of the transmitted signal to compensate for this time-base distortion allows reception of an undistorted signal. In most radar applications, an arbitrary waveform generator (AWG) would be used to store the pre-calculated waveform and then play back this waveform during transmission. The Goldstone Solar System Radar (GSSR), however, has transmission durations that exceed the available memory storage of such a device. A waveform generator capable of real-time pre-distortion of a radar waveform to a given time-base distortion function is needed.

To pre-distort the transmitted signal, both the baseband radar waveform and the RF carrier must be modified. In the GSSR, this occurs at the up-conversion mixing stage to an intermediate frequency (IF). A programmable oscillator (PO) is used to generate the IF along with a time-varying phase component that matches the time-base distortion of the RF carrier. This serves as the IF input to the waveform generator where it is mixed with a baseband radar waveform whose time-base has been distorted to match the given time-base distortion function producing the modulated IF output. An error control feedback loop is used to precisely control the time-base distortion of the baseband waveform, allowing its real-time generation.

The waveform generator produces IF modulated radar waveforms whose time-base has been pre-distorted to match a given arbitrary function. The following waveforms are supported: continuous wave (CW), frequency hopped (FH), binary phase code (BPC), and linear frequency modulation (LFM). The waveform generator takes as input an IF with a time varying phase component that matches the time-base distortion of the carrier. The waveform generator supports interconnection with deep-space network (DSN) timing and frequency standards, and is controlled through a 1 Gb/s Ethernet UDP/IP interface.

This real-time generation of a time-base distorted radar waveform for continuous transmission in a planetary radar is a unique capability.

This work was done by Kevin J. Quirk, Ferze D. Patawaran, Danh H. Nguyen, and Huy Nguyen of Caltech for NASA's Jet Propulsion Laboratory. Further information is contained in a TSP (see page 1). NPO-47730

Fast and Adaptive Lossless Onboard Hyperspectral Data Compression System

Implementation in a field-programmable gate array provides a practical, real-time system.

NASA's Jet Propulsion Laboratory, Pasadena, California

Modern hyperspectral imaging systems are able to acquire far more data than can be downlinked from a spacecraft. Onboard data compression helps to alleviate this problem, but requires a system capable of power efficiency and high throughput. Software solutions have limited throughput performance and are power-hungry. Dedicated hardware solutions can provide both high throughput and power efficiency, while taking the load off of the main processor. Thus a hardware compression system was developed. The implementation uses a field-programmable gate array (FPGA).

The implementation is based on the fast lossless (FL) compression algorithm reported in "Fast Lossless Compression of Multispectral-Image Data" (NPO-42517), *NASA Tech Briefs*, Vol. 30, No. 8 (August 2006), page 26, which achieves excellent compression performance and has low complexity. This algorithm performs predictive compression using an adaptive filtering method, and uses adaptive Golomb coding. The implementation also packetizes the coded data. The FL algorithm is well suited for implementation in hardware. In the FPGA implementation, one sample is compressed every clock cycle, which makes for a fast and practical real-time solution for space applications.

Benefits of this implementation are:
• The underlying algorithm achieves a combination of low complexity and compression effectiveness that exceeds that of techniques currently in use.
• The algorithm requires no training data or other specific information about the nature of the spectral bands for a fixed instrument dynamic range.
• Hardware acceleration provides a throughput improvement of 10 to 100 times vs. the software implementation.

A prototype of the compressor is available in software, but it runs at a speed that does not meet spacecraft requirements. The hardware implementation targets the Xilinx Virtex IV FPGAs, and makes the use of this compressor practical for Earth satellites as well as beyond-Earth missions with hyperspectral instruments.

This work was done by Nazeeh I. Aranki, Didier Keymeulen, and Matthew A. Klimesh of Caltech, and Alireza Bakhshi of B&A Engineering for NASA's Jet Propulsion Laboratory. For more information, contact iaoffice@jpl.nasa.gov. NPO-46867

Iridium Interfacial Stack — IrIS

A bondable metallization stack prevents diffusion of oxygen and gold into silicon carbide monolithically integrated circuits operating above 500 °C.

John H. Glenn Research Center, Cleveland, Ohio

Iridium Interfacial Stack (IrIS) is the sputter deposition of high-purity tantalum silicide (TaSi$_2$-400 nm) / platinum (Pt-200 nm) / iridium (Ir-200 nm) / platinum (Pt-200 nm) in an ultra-high vacuum system followed by a 600 °C anneal in nitrogen for 30 minutes. IrIS simultaneously acts as both a bond metal and a diffusion barrier. This bondable metallization that also acts as a diffusion barrier can prevent oxygen from air and gold from the wire-bond from infiltrating silicon carbide (SiC) monolithically integrated circuits (ICs) operating above 500 °C in air for over 1,000 hours. This TaSi$_2$/Pt/Ir/Pt metallization is easily bonded for electrical connection to off-chip circuitry and does not require extra anneals or masking steps.

There are two ways that IrIS can be used in SiC ICs for applications above 500 °C: it can be put directly on a SiC ohmic contact metal, such as Ti, or be used as a bond metal residing on top of an interconnect metal. For simplicity, only the use as a bond metal is discussed. The layer thickness ratio of TaSi$_2$ to the first Pt layer deposited thereon should be 2:1. This will allow Si from the TaSi$_2$ to react with the Pt to form Pt$_2$Si during the 600 °C anneal carried out after all layers have been deposited. The Ir layer does not readily form a silicide at 600 °C, and thereby prevents the Si from migrating into the top-most Pt layer during future anneals and high-temperature IC operation. The second (i.e., top-most) deposited Pt layer needs to be about 200 nm to enable easy wire bonding. The thickness of 200 nm for Ir was chosen for initial experiments; further optimization

of the Ir layer thickness may be possible via further experimentation. Ir itself is not easily wire-bonded because of its hardness and much higher melting point than Pt. Below the iridium layer, the TaSi$_2$ and Pt react and form desired Pt$_2$Si during the post-deposition anneal while above the iridium layer remains pure Pt as desired to facilitate easy and strong wire-bonding to the SiC chip circuitry.

This work was done by David Spry of Glenn Research Center. Further information is contained in a TSP (see page 1).

Inquiries concerning rights for the commercial use of this invention should be addressed to NASA Glenn Research Center, Innovative Partnerships Office, Attn: Steven Fedor, Mail Stop 4–8, 21000 Brookpark Road, Cleveland, Ohio 44135. Refer to LEW-18736-1 .

Downsampling Photodetector Array With Windowing

Applications include laser ranging for commercial surveys, and building-to-building optical data links.

NASA's Jet Propulsion Laboratory, Pasadena, California

In a photon counting detector array, each pixel in the array produces an electrical pulse when an incident photon on that pixel is detected. Detection and demodulation of an optical communication signal that modulated the intensity of the optical signal requires counting the number of photon arrivals over a given interval. As the size of photon counting photodetector arrays increases, parallel processing of all the pixels exceeds the resources available in current application-specific integrated circuit (ASIC) and gate array (GA) technology; the desire for a high fill factor in avalanche photodiode (APD) detector arrays also precludes this.

Through the use of downsampling and windowing portions of the detector array, the processing is distributed between the ASIC and GA. This allows demodulation of the optical communication signal incident on a large photon counting detector array, as well as providing architecture amenable to algorithmic changes.

The detector array readout ASIC functions as a parallel-to-serial con-

verter, serializing the photodetector array output for subsequent processing. Additional downsampling functionality for each pixel is added to this ASIC. Due to the large number of pixels in the array, the readout time of the entire photodetector is greater than the time between photon arrivals; therefore, a downsampling pre-processing step is done in order to increase the time allowed for the readout to occur. Each pixel drives a small counter that is incremented at every detected photon arrival or, equivalently, the charge in a storage capacitor is incremented. At the end of a user-configurable counting period (calculated independently from the ASIC),
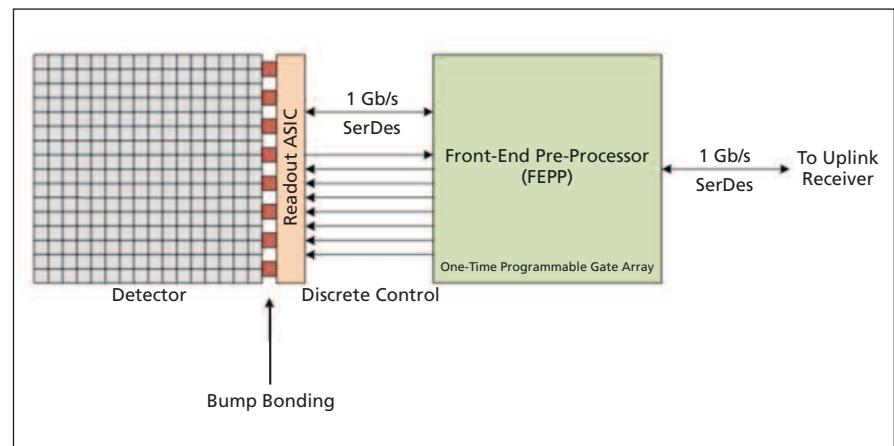
Processing can be distributed across an ASIC and GA through downsampling and windowing portions of the **Detector Array**.

the counters are sampled and cleared. This downsampled photon count information is then sent one counter word at a time to the GA.

For a large array, processing even the downsampled pixel counts exceeds the capabilities of the GA. Windowing of the array, whereby several subsets of pixels are designated for processing, is used to further reduce the computational requirements. The grouping of the designated pixel frame as the photon count information is sent one word at a time to the GA, the aggregation of the pixels in a window can be achieved by selecting only the designated pixel counts from the serial stream of photon counts, thereby obviating the need to store the entire frame of pixel count in the gate array. The pixel count sequence from each window can then be processed, forming lower-rate pixel statistics for each window. By having this processing occur in the GA rather than in the ASIC, future changes to the processing algorithm can be readily implemented.

The high-bandwidth requirements of a photon counting array combined with the properties of the optical modulation being detected by the array present a unique problem that has not been addressed by current CCD or CMOS sensor array solutions.

Optical Phase Recovery and Locking in a PPM Laser Communication Link
Coherence augmentation in a pulsed optical communication link will enable enhanced Doppler tracking and ranging capabilities.

NASA's Jet Propulsion Laboratory, Pasadena, California

Free-space optical communication holds great promise for future space missions requiring high data rates. For data communication in deep space, the current architecture employs pulse position modulation (PPM). In this scheme, the light is transmitted and detected as pulses within an array of time slots. While the PPM method is efficient for data transmission, the phase of the laser light is not utilized.

The phase coherence of a PPM optical signal has been investigated with the goal of developing a new laser communication and ranging scheme that utilizes optical coherence within the established PPM architecture and photon-counting detection (PCD). Experimental measurements of a PPM modulated optical signal were conducted, and modeling code was developed to generate random PPM signals and simulate spectra via FFT (Fast Fourier Transform) analysis. The experimental results show very good agreement with the simulations and confirm that coherence is preserved despite modulation with high extinction ratios and very low duty cycles.

A real-time technique has been developed to recover the phase information through the mixing of a PPM signal with a frequency-shifted local oscillator (LO). This mixed signal is amplified, filtered, and integrated to generate a voltage proportional to the phase of the modulated signal. By choosing an appropriate time constant for integration, one can maintain a phase lock despite long "dark" times between consecutive pulses with low duty cycle. A proof-of-principle demonstration was first achieved with an RF-based PPM signal and test setup. With the same principle method, an optical carrier within a PPM modulated laser beam could also be tracked and recovered. A reference laser was phase-locked to an independent pulsed laser signal with low-duty-cycle pseudo-random PPM codes. In this way, the drifting carrier frequency in the primary laser source is tracked via its phase change in the mixed beat note, while the corresponding voltage feedback maintains the phase lock between the two laser sources.

The novelty and key significance of this work is that the carrier phase information can be harnessed within an optical communication link based on PPM-PCD architecture. This technology development could lead to quantum-limited efficient performance within the communication link itself, as well as enable high-resolution optical tracking capabilities for planetary science and spacecraft navigation.

High-Speed Edge-Detecting Line Scan Smart Camera
This circuit reduces size and system complexity while increasing processing frame rates.

John H. Glenn Research Center, Cleveland, Ohio

A high-speed edge-detecting line scan smart camera was developed. The camera is designed to operate as a component in a NASA Glenn Research Center developed inlet shock detection system. The inlet shock is detected by projecting a laser sheet through the airflow. The shock within the airflow is the densest part and refracts the laser sheet the most in its vicinity, leaving a dark spot or shadowgraph. These spots show up as a dip or negative peak within the pixel intensity profile of an image of the projected laser sheet. The smart camera acquires and processes in real-time the linear image containing the shock shadowgraph and outputting the shock location. Previously a high-speed camera

and personal computer would perform the image capture and processing to determine the shock location.

This innovation consists of a linear image sensor, analog signal processing circuit, and a digital circuit that provides a numerical digital output of the shock or negative edge location. The smart camera is capable of capturing and processing linear images at over 1,000 frames per second. The edges are identified as numeric pixel values within the linear array of pixels, and the edge location information can be sent out from the circuit in a variety of ways, such as by using a microcontroller and onboard or external digital interface to include serial data such as RS-232/485, USB, Ethernet, or CAN BUS; parallel digital data; or an analog signal. The smart camera system can be integrated into a small package with a relatively small number of parts, reducing size and increasing reliability over the previous imaging system.

This work was done by Norman F. Prokop of Glenn Research Center. Further information is contained in a TSP (see page 1).

Inquiries concerning rights for the commercial use of this invention should be addressed to NASA Glenn Research Center, Innovative Partnerships Office, Attn: Steven Fedor, Mail Stop 4–8, 21000 Brookpark Road, Cleveland, Ohio 44135. Refer to LEW-18816-1.

Optical Communications Channel Combiner

NASA's Jet Propulsion Laboratory, Pasadena, California

NASA has identified deep-space optical communications links as an integral part of a unified space communication network in order to provide data rates in excess of 100 Mb/s. The distances and limited power inherent in a deep-space optical downlink necessitate the use of photon-counting detectors and a power-efficient modulation such as pulse position modulation (PPM). For the output of each photodetector, whether from a separate telescope or a portion of the detection area, a communication receiver estimates a log-likelihood ratio for each PPM slot. To realize the full effective aperture of these receivers, their outputs must be combined prior to information decoding.

A channel combiner was developed to synchronize the log-likelihood ratio (LLR) sequences of multiple receivers, and then combines these into a single LLR sequence for information decoding. The channel combiner synchronizes the LLR sequences of up to three receivers and then combines these into a single LLR sequence for output. The channel combiner has three channel inputs, each of which takes as input a sequence of four-bit LLRs for each PPM slot in a codeword via a XAUI 10 Gb/s quad optical fiber interface. The cross-correlation between the channels' LLR time series are calculated and used to synchronize the sequences prior to combining. The output of the channel combiner is a sequence of four-bit LLRs for each PPM slot in a codeword via a XAUI 10 Gb/s quad optical fiber interface. The unit is controlled through a 1 Gb/s Ethernet UDP/IP interface.

A deep-space optical communication link has not yet been demonstrated. This ground-station channel combiner was developed to demonstrate this capability and is unique in its ability to process such a signal.

This work was done by Kevin J. Quirk, Jonathan W. Gin, Danh H. Nguyen, and Huy Nguyen of Caltech for NASA's Jet Propulsion Laboratory. For more information, contact iaoffice@jpl.nasa.gov. NPO-47733

Development of Thermal Infrared Sensor To Supplement Operational Land Imager
The application is for the Landsat Data Continuity Mission.

Goddard Space Flight Center, Greenbelt, Maryland

The thermal infrared sensor (TIRS) is a quantum well infrared photodetector (QWIP)-based instrument intended to supplement the Operational Land Imager (OLI) for the Landsat Data Continuity Mission (LDCM). The TIRS instrument is a far-infrared imager operating in the pushbroom mode with two IR channels: 10.8 and 12 μm. The focal plane will contain three 640×512 QWIP arrays mounted onto a silicon substrate. The readout integrated circuit (ROIC) addresses each pixel on the QWIP arrays and reads out the pixel value (signal). The ROIC is controlled by the focal plane electronics (FPE) by means of clock signals and bias voltage value. The means of how the FPE is designed to control and interact with the TIRS focal plane assembly (FPA) is the basis for this work.

The technology developed under the FPE is for the TIRS focal plane assembly (FPA). The FPE must interact with the FPA to command and control the FPA, extract analog signals from the FPA, and then convert the analog signals to digital format and send them via a serial link (USB) to a computer. The FPE accomplishes the described functions by converting electrical power from generic power supplies to the required bias power that is needed by the FPA. The FPE also generates digital clocking signals and shifts the typical transistor-to-transistor logic (TTL) to ±5 V required by the FPA. The FPE also uses an application-specific integrated circuit (ASIC) named System Image, Digitizing, Enhancing, Controlling, And Retrieving (SIDECAR) from Teledyne Corp. to generate the clocking patterns commanded by the user. The uniqueness of the FPE for TIRS lies in that the TIRS FPA has three QWIP detector arrays, and all three detector arrays must be in synchronization while in operation. This is to avoid data skewing while observing

Earth flying in space. The observing scenario may be customized by uploading new control software to the SIDECAR.

Amplitude-Stabilized Oscillator for a Capacitance-Probe Electrometer

NASA's Jet Propulsion Laboratory, Pasadena, California

A multichannel electrometer voltmeter that employs a mechanical resonator maintained in sustained amplitude-stabilized oscillation has been developed for the space-based measurement of an Internal Electrostatic Discharge Monitor (IESDM) sensor. The IESDM is new sensor technology targeted for integration into a Space Environmental Monitor (SEM) subsystem used for the characterization and monitoring of deep dielectric charging on spacecraft. Creating a stable oscillator from the mechanical resonator was achieved by employing magnetic induction for sensing the resonator's velocity, and forcing a current through a coil embedded in the resonator to produce a Lorentz actuation force that overcomes the resonator's dissipative losses. Control electronics employing an AGC loop provide conditions for stabilized, constant amplitude harmonic oscillation.

The prototype resonator was composed of insulating FR4 printed-wireboard (PWB) material containing a flat, embedded, rectangular coil connected through flexure springs to a base PWB, and immersed in a magnetic field having two regions of opposite field direction generated by four neodymium block magnets. In addition to maintaining the mechanical movement needed for the electrometer's capacitor-probe transducer, this oscillator provides a reference signal for synchronous detection of the capacitor probe's output signal current so drift of oscillation frequency due to environmental effects is inconsequential.

Software

Automated Performance Characterization of DSN System Frequency Stability Using Spacecraft Tracking Data

This software provides an automated capability to measure and qualify the frequency stability performance of the Deep Space Network (DSN) ground system, using daily spacecraft tracking data. The results help to verify if the DSN performance is meeting its specification, therefore ensuring commitments to flight missions; in particular, the radio science investigations. The rich set of data also helps the DSN Operations and Maintenance team to identify the trends and patterns, allowing them to identify the antennas of lower performance and implement corrective action in a timely manner.

Unlike the traditional approach where the performance can only be obtained from special calibration sessions that are both time-consuming and require manual setup, the new method taps into the daily spacecraft tracking data. This new approach significantly increases the amount of data available for analysis, roughly by two orders of magnitude, making it possible to conduct trend analysis with good confidence.

The software is built with automation in mind for end-to-end processing. From the inputs gathering to computation analysis and later data visualization of the results, all steps are done automatically, making the data production at near zero cost. This allows the limited engineering resource to focus on high-level assessment and to follow up with the exceptions/deviations.

To make it possible to process the continual stream of daily incoming data without much effort, and to understand the results quickly, the processing needs to be automated and the data summarized at a high level. Special attention needs to be given to data gathering, input validation, handling anomalous conditions, computation, and presenting the results in a visual form that makes it easy to spot items of exception/deviation so that further analysis can be directed and corrective actions followed.

This work was done by Timothy T. Pham, Richard J. Machuzak, Alina Bedrossian, Richard M. Kelly, and Jason C. Liao of Caltech for NASA's Jet Propulsion Laboratory.

For more information, contact iaoffice @jpl.nasa.gov.

This software is available for commercial licensing. Please contact Daniel Broderick of the California Institute of Technology at danielb@caltech.edu. Refer to NPO-47532.

Histogrammatic Method for Determining Relative Abundance of Input Gas Pulse

To satisfy the Major Constituents Analysis (MCA) requirements for the Vehicle Cabin Atmosphere Monitor (VCAM), this software analyzes the relative abundance ratios for N_2, O_2, Ar, and CO_2 as a function of time and constructs their best-estimate mean. A histogram is first built of all abundance ratios for each of the species vs time. The abundance peaks corresponding to the intended measurement and any obfuscating background are then separated via standard peak-finding techniques in histogram space. A voting scheme is then used to include/exclude this particular time sample in the final average based on its membership to the intended measurement or the background population. This results in a robust and reasonable estimate of the abundance of trace components such as CO_2 and Ar even in the presence of obfuscating backgrounds internal to the VCAM device.

VCAM can provide a means for monitoring the air within the enclosed environments, such as the ISS (International Space Station), Crew Exploration Vehicle (CEV), a Lunar Habitat, or another vehicle traveling to Mars. Its miniature pre-concentrator, gas chromatograph (GC), and mass spectrometer can provide unbiased detection of a large number of organic species as well as MCA analysis. VCAM's software can identify the concentration of trace chemicals and whether the chemicals are on a targeted list of hazardous compounds. This innovation's performance and reliability on orbit, along with the ground team's assessment of its raw data and analysis results, will validate its technology for future use and development.

This work was done by Lukas Mandrake, Benjamin J. Bornstein, Stojan Madzunkov, and John A. MacAskill of Caltech for NASA's Jet Propulsion Laboratory.

This software is available for commercial licensing. Please contact Daniel Broderick of the California Institute of Technology at danielb@caltech.edu. Refer to NPO-47217.

Predictive Sea State Estimation for Automated Ride Control and Handling — PSSEARCH

PSSEARCH provides predictive sea state estimation, coupled with closed-loop feedback control for automated ride control. It enables a manned or unmanned watercraft to determine the 3D map and sea state conditions in its vicinity in real time. Adaptive path-planning/replanning software and a control surface management system will then use this information to choose the best settings and heading relative to the seas for the watercraft.

PSSEARCH looks ahead and anticipates potential impact of waves on the boat and is used in a tight control loop to adjust trim tabs, course, and throttle settings. The software uses sensory inputs including IMU (Inertial Measurement Unit), stereo, radar, etc. to determine the sea state and wave conditions (wave height, frequency, wave direction) in the vicinity of a rapidly moving boat. This information can then be used to plot a "safe" path through the oncoming waves.

The main issues in determining a safe path for sea surface navigation are: (1) deriving a 3D map of the surrounding environment, (2) extracting hazards and sea state surface state from the imaging sensors/map, and (3) planning a path and control surface settings that avoid the hazards, accomplish the mission navigation goals, and mitigate crew injuries from excessive heave, pitch, and roll accelerations while taking into account the dynamics of the sea surface state. The first part is solved using a wide baseline stereo system, where 3D structure is determined from two calibrated pairs of visual imagers.

Once the 3D map is derived, anything above the sea surface is classified as a potential hazard and a surface analysis gives a static snapshot of the waves. Dynamics of the wave features are obtained from a frequency analysis of motion vectors derived from the orientation of the waves during a sequence of inputs. Fusion of the dynamic wave patterns with the 3D maps and the IMU outputs is used for efficient safe path planning.

⟩ LEGION: Lightweight Expandable Group of Independently Operating Nodes

LEGION is a lightweight C-language software library that enables distributed asynchronous data processing with a loosely coupled set of compute nodes. Loosely coupled means that a node can offer itself in service to a larger task at any time and can withdraw itself from service at any time, provided it is not actively engaged in an assignment. The main program, i.e., the one attempting to solve the larger task, does not need to know up front which nodes will be available, how many nodes will be available, or at what times the nodes will be available, which is normally the case in a "volunteer computing" framework. The LEGION software accomplishes its goals by providing message-based, inter-process communication similar to MPI (message passing interface), but without the tight coupling requirements. The software is lightweight and easy to install as it is written in standard C with no exotic library dependencies.

LEGION has been demonstrated in a challenging planetary science application in which a machine learning system is used in closed-loop fashion to efficiently explore the input parameter space of a complex numerical simulation. The machine learning system decides which jobs to run through the simulator; then, through LEGION calls, the system farms those jobs out to a collection of compute nodes, retrieves the job results as they become available, and updates a predictive model of how the simulator maps inputs to outputs. The machine learning system decides which new set of jobs would be most informa-

tive to run given the results so far; this basic loop is repeated until sufficient insight into the physical system modeled by the simulator is obtained.

⟩ Real-Time Projection to Verify Plan Success During Execution

The Mission Data System provides a framework for modeling complex systems in terms of system behaviors and goals that express intent. Complex activity plans can be represented as goal networks that express the coordination of goals on different state variables of the system. Real-time projection extends the ability of this system to verify plan achievability (all goals can be satisfied over the entire plan) into the execution domain so that the system is able to continuously re-verify a plan as it is executed, and as the states of the system change in response to goals and the environment.

Previous versions were able to detect and respond to goal violations when they actually occur during execution. This new capability enables the prediction of future goal failures; specifically, goals that were previously found to be achievable but are no longer achievable due to unanticipated faults or environmental conditions. Early detection of such situations enables operators or an autonomous fault response capability to deal with the problem at a point that maximizes the available options.

For example, this system has been applied to the problem of managing battery energy on a lunar rover as it is used to explore the Moon. Astronauts drive the rover to waypoints and conduct science observations according to a plan that is scheduled and verified to be achievable with the energy resources available. As the astronauts execute this plan, the system uses this new capability to continuously re-verify the plan as energy is consumed to ensure that the battery will never be depleted below safe levels across the entire plan.

In particular, this enables an execution system to predict problems such as resource exhaustion before they occur. The models are expressed and executed in a way that can be optimized for real-

time use in an embedded system.

⟩ Automated Performance Characterization of DSN System Frequency Stability Using Spacecraft Tracking Data

This software provides an automated capability to measure and qualify the frequency stability performance of the Deep Space Network (DSN) ground system, using daily spacecraft tracking data. The results help to verify if the DSN performance is meeting its specification, therefore ensuring commitments to flight missions; in particular, the radio science investigations. The rich set of data also helps the DSN Operations and Maintenance team to identify the trends and patterns, allowing them to identify the antennas of lower performance and implement corrective action in a timely manner.

Unlike the traditional approach where the performance can only be obtained from special calibration sessions that are both time-consuming and require manual setup, the new method taps into the daily spacecraft tracking data. This new approach significantly increases the amount of data available for analysis, roughly by two orders of magnitude, making it possible to conduct trend analysis with good confidence.

The software is built with automation in mind for end-to-end processing. From the inputs gathering to computation analysis and later data visualization of the results, all steps are done automatically, making the data production at near zero cost. This allows the limited engineering resource to focus on high-level assessment and to follow up with the exceptions/deviations.

To make it possible to process the continual stream of daily incoming data without much effort, and to understand the results quickly, the processing needs to be automated and the data summarized at a high level. Special attention needs to be given to data gathering, input validation, handling anomalous conditions, computation, and present-

ing the results in a visual form that makes it easy to spot items of exception/deviation so that further analysis can be directed and corrective actions followed.

∑ Web-Based Customizable Viewer for Mars Network Overflight Opportunities

This software displays a full summary of information regarding the overflight opportunities between any set of lander and orbiter pairs that the user has access to view. The information display can be customized, allowing the user to choose which fields to view/hide and filter.

The software works from a Web browser on any modern operating system. A full summary of information pertaining to an overflight is available, including the proposed, tentative, requested, planned, and implemented. This gives the user a chance to quickly check for inconsistencies and fix any problems.

Overflights from multiple lander/orbiter pairs can be compared instantly, and information can be filtered through the query and shown/hidden, giving the user a customizable view of the data. The information can be exported to a CSV (comma separated value) or XML (extensible markup language) file. The software only grants access to users who are authorized to view the information.

This application is an addition to the MaROS Web suite. Prior to this addition, information pertaining to overflight opportunities would have a limited amount of data (displayed graphically) and could only be shown in strict temporal ordering. This new display shows more information, allows direct comparisons between overflights, and allows the data to be manipulated in ways that it was unable to be done in the past.

The current software solution is to use CSV files to view the overflight opportunities.

Fabrication of a Cryogenic Terahertz Emitter for Bolometer Focal Plane Calibrations

The methods used produce an emitter that features greater precision.

Goddard Space Flight Center, Greenbelt, Maryland

A fabrication process is reported for prototype emitters of THz radiation, which operate cryogenically, and should provide a fast, stable blackbody source suitable for characterization of THz devices. The fabrication has been demonstrated and, at the time of this reporting, testing was underway. The emitter is similar to a monolithic silicon bolometer in design, using both a low-noise thermometer and a heater element on a thermally isolated stage. An impedance-matched, high-emissivity coating is also integrated to tune the blackbody properties.

This emitter is designed to emit a precise amount of power as a blackbody spectrum centered on terahertz frequencies. The emission is a function of the blackbody temperature. An integrated resistive heater and thermometer system can control the temperature of the blackbody with greater precision than previous incarnations of calibration sources that relied on blackbody emission.

The emitter is fabricated using a silicon-on-insulator substrate wafer. The buried oxide is chosen to be less than 1 micron thick, and the silicon device thickness is 1–2 microns. Layers of phosphorus compensated with boron are implanted into and diffused throughout the full thickness of the silicon device layer to create the thermometer and heater components. Degenerately doped wiring is implanted to connect the devices to wire-bondable contact pads at the edge of the emitter chip. Then the device is micromachined to remove the thick-handle silicon behind the thermometer and heater components, and to thermally isolate it on a silicon membrane. An impedance-matched emissive coating (ion assisted evaporated Bi) is applied to the back of the membrane to enable high-efficiency emission of the blackbody spectrum.

In operation, the heater is supplied with a voltage that is PID-controlled (proportional-integral-derivative-controlled) by the output of the thermometer. Both components are quiet, and require low-noise readout and power supplies to function correctly. The fabricated chip is mounted and heat-sunk to a copper housing that directs and collimates the beam of terahertz power emitted from the chip. Filtering in the optical column in the copper housing with metal mesh or neutral density components is also possible. The implanted silicon is highly reliable and stable. The Bi coating is robust but may require passivation if the environment for installation has corrosives (i.e., acid flux, heavy solvents from a Dewar).

This work was done by James Chervenak, Ari Brown, and Edward Wollack of Goddard Space Flight Center. Further information is contained in a TSP (see page 1). GSC-16131-1

Fabrication of an Absorber-Coupled MKID Detector

This allows for multiplexed microwave readout and, consequently, good spatial discrimination between pixels in the array.

Goddard Space Flight Center, Greenbelt, Maryland

Absorber-coupled microwave kinetic inductance detector (MKID) arrays were developed for submillimeter and far-infrared astronomy. These sensors comprise arrays of lambda/2 stepped microwave impedance resonators patterned on a 1.5-mm-thick silicon membrane, which is optimized for optical coupling. The detector elements are supported on a 380-mm-thick micro-machined silicon wafer. The resonators consist of parallel plate aluminum transmission lines coupled to low-impedance Nb microstrip traces of variable length, which set the resonant frequency of each resonator. This allows for multiplexed microwave readout and, conse-

quently, good spatial discrimination between pixels in the array. The transmission lines simultaneously act to absorb optical power and employ an appropriate surface impedance and effective filling fraction. The fabrication techniques demonstrate high-fabrication yield of MKID arrays on large, single-crystal membranes and sub-micron front-to-back alignment of the microstrip circuit.

An MKID is a detector that operates upon the principle that a superconducting material's kinetic inductance and surface resistance will change in response to being exposed to radiation with a power density sufficient to break its Cooper pairs. When integrated as

part of a resonant circuit, the change in surface impedance will result in a shift in its resonance frequency and a decrease of its quality factor. In this approach, incident power creates quasiparticles inside a superconducting resonator, which is configured to match the impedance of free space in order to absorb the radiation being detected. For this reason MKIDs are attractive for use in large-format focal plane arrays, because they are easily multiplexed in the frequency domain and their fabrication is straightforward.

The fabrication process can be summarized in seven steps: (1) Alignment marks are lithographically patterned

and etched all the way through a silicon on insulator (SOI) wafer, which consists of a thin silicon membrane bonded to a thick silicon handle wafer. (2) The metal microwave circuitry on the front of the membrane is patterned and etched. (3) The wafer is then temporarily bonded with wafer wax to a Pyrex wafer, with the SOI side abutting the Pyrex. (4) The silicon handle component of the SOI wafer is subsequently etched away so as to expose the membrane backside. (5) The wafer is flipped over, and metal microwave circuitry is patterned and etched on the membrane backside. Furthermore, cuts in the membrane are made so as to define the individual detector array chips. (6) Silicon frames are micromachined and glued to the silicon membrane. (7) The membranes, which are now attached to the frames, are released from the Pyrex wafer via dissolution of the wafer wax in acetone.

Graphene Transparent Conductive Electrodes for Next-Generation Microshutter Arrays

Goddard Space Flight Center, Greenbelt, Maryland

Graphene is a single atomic layer of graphite. It is optically transparent and has high electron mobility, and thus has great potential to make transparent conductive electrodes. This invention contributes towards the development of graphene transparent conductive electrodes for next-generation microshutter arrays.

The original design for the electrodes of the next generation of microshutters uses indium-tin-oxide (ITO) as the electrode material. ITO is widely used in NASA flight missions. The optical transparency of ITO is limited, and the material is brittle. Also, ITO has been getting more expensive in recent years. The objective of the invention is to develop a graphene transparent conductive electrode that will replace ITO. An exfoliation procedure was developed to make graphene out of graphite crystals. In addition, large areas of single-layer graphene were produced using low-pressure chemical vapor deposition (LPCVD) with high optical transparency. A special graphene transport procedure was developed for transferring graphene from copper substrates to arbitrary substrates.

The concept is to grow large-size graphene sheets using the LPCVD system through chemical reaction, transfer the graphene film to a substrate, dope graphene to reduce the sheet resistance, and pattern the film to the dimension of the electrodes in the microshutter array.

Graphene transparent conductive electrodes are expected to have a transparency of 97.7%. This covers the electromagnetic spectrum from UV to IR. In comparison, ITO electrodes currently used in microshutter arrays have 85% transparency in mid-IR, and suffer from dramatic transparency drop at a wavelength of near-IR or shorter. Thus, graphene also has potential application as transparent conductive electrodes for Schottky photodiodes in the UV region.

Method of Bonding Optical Elements With Near-Zero Displacement

Displacement caused by epoxy shrinking as it cures is reduced less than 200 nm.

Goddard Space Flight Center, Greenbelt, Maryland

The International X-ray Project seeks to build an x-ray telescope using thousands of pieces of thin and flexible glass mirror segments. Each mirror segment must be bonded into a housing in nearly perfect optical alignment without distortion. Forces greater than 0.001 Newton, or displacements greater than 0.5 µm of the glass, cause unacceptable optical distortion. All known epoxies shrink as they cure. Even the epoxies with the least amount of shrinkage (<0.01%) cause unacceptable optical distortion and misalignment by pulling the mirror segments towards the housing as it cures. A related problem is that the shrinkage is not consistent or predictable so that it cannot be accounted for in the setup (i.e., if all of the bonds shrunk an equal amount, there would be no problem).

A method has been developed that allows two components to be joined with epoxy in such a way that reduces the displacement caused by epoxy shrinking as it cures to less than 200 nm. The method involves using ultraviolet-cured epoxy with a displacement sensor and a nano-actuator in a control loop. The epoxy is cured by short-duration exposures to UV light. In between each exposure, the nano-actuator zeroes out the displacement caused by epoxy shrinkage and thermal expansion. After a few exposures, the epoxy has cured sufficiently to prevent further displacement of the two components.

Bonding of optical elements has been done for many years, but most optics are thick and rigid elements that resist micro-Newton-level forces without causing distortion. When bonding thin glass optics such as the 0.40-mm thick IXO X-ray mirrors, forces in the micro- and milli-Newton levels cause unacceptable optical figure error. This innovation can now repeatedly and reliably bond a thin glass mirror to a metal housing with less than 0.2 µm of displacement (<200 nm).

This is an enabling technology that allows the installation of virtually stress-

free, undistorted thin optics onto structures. This innovation is applicable to the bonding of thin optical elements, or any thin/flexible structures, that must be attached in an undistorted, consistent, and aligned way.

This work was done by David Robinson of Goddard Space Flight Center and Ryan McClelland, Glenn Byron, and Tyler Evans of SGT, Inc.Further information is contained in a TSP (see page 1).GSC-16110-1

Free-Mass and Interface Configurations of Hammering Mechanisms

These mechanisms are applicable for construction or other industries requiring drills or actuators.

NASA's Jet Propulsion Laboratory, Pasadena, California

A series of free-mass designs for the ultrasonic/sonic driller/corer (USDC) has been developed to maximize the transfer of energy from the piezoelectric transducer through the horn to the bit, as well as to minimize potential jamming. A systematic development was made producing novel designs of free-mass configurations where the impact force is spread across a minimal area maximizing the impact on the bit. The designed free masses were made to operate at high temperatures (500 °C) as on Venus, and they can be made to operate at extremely low temperature, too.

In normal operation, the free mass bounces between the horn and the bit, impacting both repeatedly. The impact stress profile, maximum stress, contact time duration, and the required yielding stress for the materials of the free mass, bit, and horn are all affected by the contact area. A larger contact area results in lower stress in the contact region, and avoids yielding of the materials. However, before the excitation voltage is applied to the transducer, the horn, free mass, and the bit are pressed together. Larger contact area results in a stronger coupling of the bit to the horn transducer, which greatly changes the vibration characteristics of the transducer, and makes the USDC difficult to start.
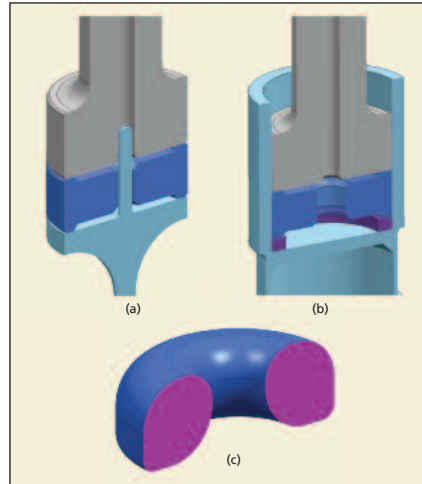
In the improved **USDC Design**, the rod was eliminated, and a solid cylinder-shaped free mass retained with a "cup" was used. On the left (a) is shown the rod configuration for the retention of the free mass, and on the right (b) the cup configuration is shown for the free mass retention. Part (c) shows a free mass with flat and curved contact areas.

To obtain optimum performance, a catalog of free-mass designs is required, allowing maximum flexibility during trade-off for these conflicting contact area requirements.

For this purpose, seven different designs were conceived: point contacts, circular contacts, point/circular contacts, line contacts, ring contacts, line/ring contacts, and dashed line contacts. Besides point/circular and line/ring contacts, the free mass can be designed as any of the above shapes. Depending on the ratio of the diameter to the height, and the free-mass retention method used (the cup or rod), the free mass can be configured with one or more sliding surfaces on the outside or inside diameter surface or both. Matching horn tips and free mass may also offer some utility in maximizing the stress pulse.

Wavefront Compensation Segmented Mirror Sensing and Control

Six degrees of freedom can be sensed at each segment edge.

NASA's Jet Propulsion Laboratory, Pasadena, California

The primary mirror of very large submillimeter-wave telescopes will necessarily be segmented into many separate mirror panels. These panels must be continuously co-phased to keep the telescope wavefront error less than a small fraction of a wavelength, to ten microns RMS (root mean square) or less. This performance must be maintained continuously across the full aperture of the telescope, in all pointing conditions, and in a variable thermal environment.

A wavefront compensation segmented mirror sensing and control system, consisting of optical edge sensors, Wavefront Compensation Estimator/Controller Software, and segment position actuators is proposed. Optical edge sensors are placed two per each segment-to-segment edge to continuously measure changes in segment state. Segment position actuators (three per segment) are used to move the panels. A computer control system uses the edge sensor

measurements to estimate the state of all of the segments and to predict the wavefront error; segment actuator commands are computed that minimize the wavefront error.

Translational or rotational motions of one segment relative to the other cause lateral displacement of the light beam, which is measured by the imaging sensor. For high accuracy, the collimator uses a shaped mask, such as one or more slits, so that the light beam forms a pattern on the sensor that permits sensing accuracy of better than 0.1 micron in two axes: in the z or local surface normal direction, and in the y direction parallel to the mirror surface and perpendicular to the beam direction.

Using a coaligned pair of sensors, with the location of the detector and collimated light source interchanged, four degrees of freedom can be sensed: transverse x and y displacements, as well as two bending angles (pitch and yaw). In this approach, each optical edge sensor head has a collimator and an imager, placing one sensor head on each side of a segment gap, with two parallel light beams crossing the gap.

Two sets of optical edge sensors are used per segment-to-segment edge, separated by a finite distance along the segment edge, for four optical heads, each with an imager and a collimator. By orienting the beam direction of one edge sensor pair to be +45° away from the segment edge direction, and the other sensor pair to be oriented –45° away from the segment edge direction, all six degrees of freedom of relative motion between the segments can be measured with some redundancy.

The software resides in a computer that receives each of the optical edge sensor signals, as well as telescope pointing commands. It feeds back the edge sensor signals to keep the primary mirror figure within specification. It uses a feed-forward control to compensate for global effects such as decollimation of the primary and secondary mirrors due to gravity sag as the telescope pointing changes to track science objects.

Three segment position actuators will be provided per segment to enable controlled motions in the piston, tip, and tilt degrees of freedom. These actuators are driven by the software, providing the optical changes needed to keep the telescope phased.

A novel aspect of this design is the angled optical edge sensor configuration. By angling the light beam of each edge sensor pair at + and –45°, a full four degrees of freedom can be sensed at each segment edge by each sensor pair. This configuration results in full observability of the segment optical state, and is crucial in achieving the needed performance.

The software incorporates a structural/optical model of the telescope in a least-squares or Kalman filter-based estimator/controller, which processes the optical edge sensor signals in a low-bandwidth control loop. The estimator produces an estimate of the optical state of the mirror, and predicts the resulting wavefront error, balancing current against previous measurements in a least-squares optimization. The controller calculates the segment actuator commands that will minimize not the sensor signals, but the predicted wavefront error. This formulation allows the controller to compensate for the optical effects of motions (such as lateral sag of the segments) that are not directly actuated. The result is far better performance than could be achieved using a conventional sensor-nulling approach.

⚙ Long-Life, Lightweight, Multi-Roller Traction Drives for Planetary Vehicle Surface Exploration
These drives can be used for Earth-based applications where extreme temperatures are involved.

John H. Glenn Research Center, Cleveland, Ohio

NASA's initiative for Lunar and Martian exploration will require long lived, robust drive systems for manned vehicles that must operate in hostile environments. The operation of these mechanical drives will pose a problem because of the existing extreme operating conditions. Some of these extreme conditions include operating at a very high or very cold temperature, operating over a wide range of temperatures, operating in very dusty environments, operating in a very high radiation environment, and operating in possibly corrosive environments.

Current drive systems use gears with various configurations of "teeth." These gears must be lubricated with oil (or grease) and must have some sort of a lubricant resupply system. For drive systems, oil poses problems such as evaporation, becoming too viscous and eventually freezing at cold temperatures, being too thin to lubricate at high temperatures, being degraded by the radiation environment, being contaminated by the regolith (soil), and if vaporized (and not sealed), it will contaminate the regolith. Thus, it may not be advisable or even possible to use oil because of these limitations.

An oil-less, compact traction vehicle drive is a drive designed for use in hostile environments like those that will be encountered on planetary surfaces. Initially, traction roller tests in vacuum were conducted to obtain traction and endurance data needed for designing the drives. From that data, a traction drive was designed that would fit into a prototype lunar rover vehicle, and this design data was used to construct several traction drives. These drives were then tested in air to determine their performance characteristics, and if any final corrections to the designs were necessary.

A limitation with current speed reducer systems such as planetary gears and harmonic drives is the high-contact stresses that occur at tooth engagement and in the harmonic drive wave generator interface. These high stresses induce high wear of solid lubricant coatings, thus necessitating the use of liquid lubricants for long life.

Because of their near-pure rolling contact, traction drives can operate unlubricated at very cold temperatures or

at high temperatures by using low-wear, high-traction materials or coatings. Oilless traction drives will not encounter the temperature swing problems of other proposed planetary vehicle drives. Traction drives also will be less sensitive to dusty conditions if sealed properly, and will also not contaminate a planetary environment because there is no liquid lubricant used.

The oil-free traction drive is a "toothless" drive system that is capable of dry operation using low-wear, high-friction mate-

rials and coatings. Multi-roller traction drive configurations offer high reduction ratios (>30 to 1) in a single stage, reducing motor size and providing a lightweight wheel drive system.

A traction drive with nearly pure rolling action provides much longer life than could be achieved with gear or harmonic drive systems in applications where liquid lubricants could not be used. Use of ceramic-coated titanium or polymer rollers will reduce the weight of the drives and also reduce the cost to launch.

✿ Reliable Optical Pump Architecture for Highly Coherent Lasers Used in Space Metrology Applications

This design also can be used in scientific instrumentation where repair is difficult such as in underwater deployment.

NASA's Jet Propulsion Laboratory, Pasadena, California

The design and initial demonstration of a laser pump module (LPM) incorporating single-mode, grating-stabilized 808-nm diode lasers and a low-loss, high-port-count optical combiner are completed. The purpose of the developed LPM is to reliably pump an Nd:YAG crystal in the laser head (LH), which serves as the optical metrology source for SIM-Lite mission. Using the narrow-linewidth, single-mode laser diodes enables placement of the pump power near Nd adsorption peak, which enhances pumping efficiency. Grating stabilization allows for stable pump spectra as diode operating temperature and bias current change. The low-loss, high-port-count optical combiner enables efficient combining of tens of pumps. Overall, the module supports 5+ years of continuous operation at 2 W of pump power with reliability approaching 100 percent.

The LPM consists of a laser diode farm (LDF) and a pump beam combiner (PBC). An array of 807- to 808-nm fiber-pigtailed laser diodes makes up the LDF. A Bragg grating in each 5-μm core single-mode (SM) fiber pigtail acts to stabilize the lasing spectra over a range of diode operating conditions. These commercially available single-mode laser diodes can deliver up to 150 mW of optical power. The outputs from the multiple pumps in the LDF are routed to the PBC, which is a 37-input by 1-output all-fiber device. The input ports consist of 5-μm core SM fiber, while the output port consists of 105-μm core, 0.15 NA (numerical aperture) multi-mode (MM)
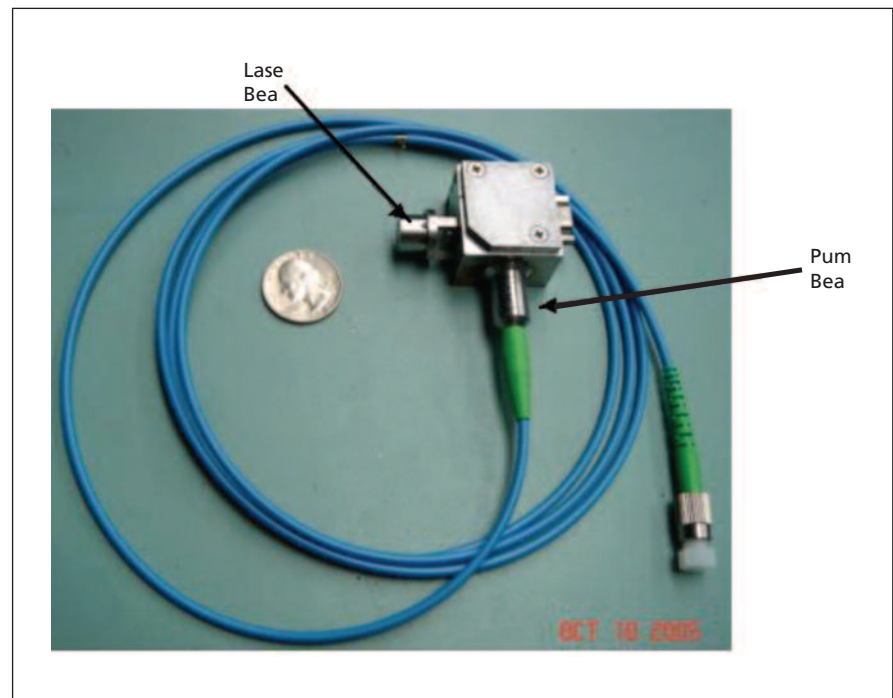
Picture of SIM-lite NPRO based LH. The optical pump is delivered to the NPRO via multimode optical fiber. The laser beam is free spaced coupled to remainder of metrology system.

fiber. The combiner is fabricated by fusing the 37 input fibers while simultaneously tapering the fused region. At the completion of this process, the MM fiber is spliced to the end of the adiabatic taper, and, for protection, the combiner is sheathed by a capillary tube. A compact and robust metal housing was designed and fabricated to protect the PBC during space deployment.

Finally, the combined pump light is delivered to the LH via MM optical fiber. Within the head, the pump beam optical train matches the pump beam to the lasing mode profile, which enhances pumping efficiency. The LH houses non-planar resonant oscillator (NPRO), and provides all conditioning necessary for proper NPRO operation. Two large magnets ensure unidirectional propagation through

the ring, mitigating hole burning. A set of heaters enables slow NPRO frequency tuning, while a piezoelectric transducer enables fast tuning. LH produces 300 mW at 1,319 nm when pumped by 1.9 W at 808 nm.

A software package predicting LDF reliability during the mission lifetime was developed based on the reliability theory of diode lasers. Extensive numerical simulations were carried out to select LDF architecture that meets the stringent reliability requirement (>99.7% probability of successful operation over 5.5 years), while balancing the competing needs to keep the number of laser diodes manageable and their operating temperature as close to room temperature as possible. Detailed sensitivity studies were also performed to make sure that the selected architecture is not vulnerable to possible deviations of key diode and mission parameters from their assumed values. The LDF architecture that was ultimately chosen meets the reliability requirements with 37 pump laser diodes operating at –1 °C (or –5 °C for an extra margin of safety).

Electrochemical Ultracapacitors Using Graphitic Nanostacks

Applications include cell phones and other portable consumer electronic devices, hybrid electric vehicles, automatic electronic defibrillators, and uninterruptable power supplies.

John H. Glenn Research Center, Cleveland, Ohio

Electrochemical ultracapacitors (ECs) have been developed using graphitic nanostacks as the electrode material. The advantages of this technology will be the reduction of device size due to superior power densities and relative powers compared to traditional activated carbon electrodes. External testing showed that these materials display reduced discharge response times compared to state-of-the-art materials. Such applications are advantageous for pulsed power applications such as burst communications (satellites, cell phones), electromechanical actuators, and battery load leveling in electric vehicles. These carbon nanostructures are highly conductive and offer an ordered mesopore network. These attributes will provide more complete electrolyte wetting, and faster release of stored charge compared to activated carbon.

Electrochemical capacitor (EC) electrode materials were developed using commercially available nanomaterials and modifying them to exploit their energy storage properties. These materials would be an improvement over current ECs that employ activated carbon as the electrode material. Commercially available graphite nanofibers (GNFs) are used as precursor materials for the synthesis of graphitic nanostacks (GNSs). These materials offer much greater surface area than graphite flakes. Additionally, these materials offer a superior electrical conductivity and a greater average pore size compared to activated carbon electrodes.

The state of the art in EC development uses activated carbon (AC) as the electrode material. AC has a high surface area, but its small average pore size inhibits electrolyte ingress/egress. Additionally, AC has a higher resistivity, which generates parasitic heating in high-power applications. This work focuses on fabricating EC from carbon that has a very different structure by increasing the surface area of the GNF by intercalation or exfoliation of the graphitic basal planes. Additionally, various functionalities to the GNS surface will be added that can exhibit pseudocapacitance. This pseudocapacitance exhibits faradaic (charge transfer) properties that can further increase the overall relative and volumetric capacitance of the material.

A process is also proposed to use GNF as a precursor material to fabricate GNS that will be used as EC electrodes. This results in much better electrical conductivity than activated carbon. This is advantageous for high-pulsed-power applications to reduce parasitic heating. Larger average pore size allows more complete electrolyte wetting (faster charge transfer kinetics). These properties contribute to a lowered equivalent series resistance (ESR), increased specific power, shorter charging times, and decreased parasitic heating. The high density of basal plane edges provides nucleation sites for activation (addition of hydrophilic functional groups) that facilitate electrolyte wetting, and will contribute to pseudocapacitance.

Improved Whole-Blood-Staining Device

Additional applications have been identified.

Lyndon B. Johnson Space Center, Houston, Texas

Dramatic improvements have been made in NASA's Whole Blood Staining Device (WBSD) since it was last described in "Whole-Blood-Staining Device," *NASA Tech Briefs*, Vol. 23, No. 10 (October 1999), page 64. The new system has a longer shelf life, a simpler and more effective operational procedure, improved interface with instrumentation, and shorter processing time. More specifically, the improvements have targeted bag and locking clip materials, sampling ports, and air pocket prevention.

The WBSD stains whole blood collected during spaceflight for subsequent flow cytometric analysis. In short, the main device stains white blood cells by use of monoclonal antibodies conjugated to various fluorochromes, followed by lysing and fixing of the cells by use of a commercial reagent that has been diluted according to NASA safety standards. This system is compact, robust, and does not require electric power, precise mixing, or precise incubation times.

Figure 1 depicts the present improved version for staining applications, which is a poly(tetrafluoroethylene) bag with a Luer-lock port and plastic locking clips. An InterLink® (or equivalent) intravenous-injection port screws into the Luer-lock port. The inflatable/collapsible nature of the bag facilitates loading and helps to minimize the amount of air trapped in the fully loaded bag.

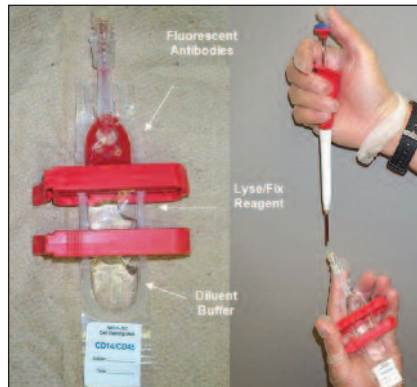Some additional uses have been identified for the device beyond whole blood

Figure 1. Photo of the **Improved Version** for staining applications.

staining. The WBSD has been configured for functional assays that require culture of live cells by housing sterile culture media, mitogens, and fixatives prior to use [Figure 2(a)]. Simple injection of whole blood allows cell-stimulation culture to be performed in reduced gravity conditions, and product stabilization prior to storage, while protecting astronauts from liquid biohazardous materials. Also, the improved WBSD has reconstituted powdered injectable antibiotics by mixing them with diluent liquids [Figure 2(b)]. Although such mixing can readily be performed on Earth by shaking in glass vials, it cannot readily be performed this way in outer space without entraining air bubbles. The present device can be preloaded with the powder and diluent(s) in separate
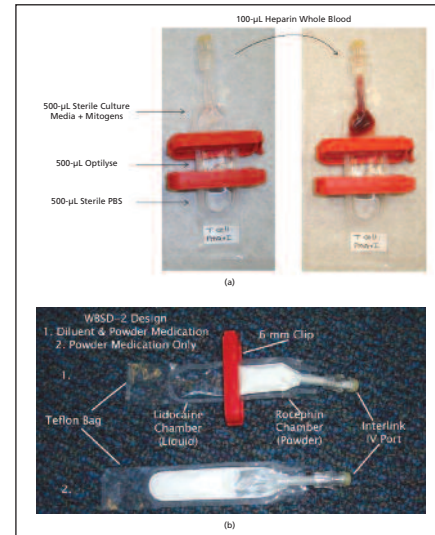
Figure 2. **WBSD Configurations**: (a) for functional assays, and (b) for powdered injectable antibiotics.

compartments. The powder and diluent(s) can be mixed, without introducing air bubbles, by removing the clip(s), then shaking. This use of the device could also be advantageous in terrestrial applications because it maintains the isolation of the constituents until the time of use.

This work was done by Clarence F. Sams of Johnson Space Center and Brian Crucian, Bonnie Paul, Shannon Melton, and Terry Guess of Wyle Laboratories. Further information is contained in a TSP (see page 1). MSC-24176-1/7-1/8-1

Monitoring Location and Angular Orientation of a Pill

System is part of targeted drug delivery.

Ames Research Center, Moffett Field, California

A mobile pill transmitter system moves through, or adjacent to, one or more organs in an animal or human body, while transmitting signals from its present location and/or present angular orientation. The system also provides signals from which the present roll angle of the pill,

about a selected axis, can be determined. When the location coordinates angular orientation and the roll angle of the pill are within selected ranges, an aperture on the pill container releases a selected chemical into, or onto, the body. Optionally, the pill, as it moves, provides a se-

quence of visually perceptible images. The times for image formation may correspond to times at which the pill transmitter system location or image satisfies one of at least four criteria.

This invention provides and supplies an algorithm for exact determination of

location coordinates and angular orientation coordinates for a mobile pill transmitter (PT), or other similar device that is introduced into, and moves within, a GI tract of a human or animal body. A set of as many as eight nonlinear equations has been developed and applied, relating propagation of a wireless signal between either two, three, or more transmitting antennas located on the PT, to four or more non-coplanar receiving antennas located on a signal receiver appliance worn by the user.

The equations are solved exactly, without approximations or iterations, and are applied in several environments: (1) association of a visual image, transmitted by the PT at each of a second sequence of times, with a PT location and PT angular orientation at that time; (2) determination of a position within the body at which a drug or chemical substance or other treatment is to be delivered to a selected portion of the body; (3) monitoring, after delivery, of the effect(s) of administration of the treatment; and (4) determination of one or more positions within the body where provision and examination of a finer-scale image is warranted.

This work was done by John F. Schipper for Ames Research Center. Further information is contained in a TSP (see page 1). ARC-15810-1

Molecular Technique to Reduce PCR Bias for Deeper Understanding of Microbial Diversity

This technique has applications in medical manufacturing, food processing, and municipal water treatment.

NASA's Jet Propulsion Laboratory, Pasadena, California

Current planetary protection policies require that spacecraft targeted to sensitive solar system bodies be assembled and readied for launch in controlled cleanroom environments. A better understanding of the distribution and frequency at which high-risk contaminant microbes are encountered on spacecraft surfaces would significantly aid in assessing the threat of forward contamination. However, despite a growing understanding of the diverse microbial populations present in cleanrooms, less abundant microbial populations are probably not adequately taken into account due to technological limitations. This novel approach encompasses a wide spectrum of microbial species and will represent the true picture of spacecraft cleanroom-associated microbial diversity.

All of the current microbial diversity assessment techniques are based on an initial PCR amplification step. However, a number of factors are known to bias PCR amplification and jeopardize the true representation of bacterial diversity. PCR amplification of a minor template appears to be suppressed by the amplification of a more abundant template. It is widely acknowledged among environmental molecular microbiologists that genetic biosignatures identified from an environment only represent the most dominant populations. The technological bottleneck overlooks the presence of the less abundant minority population and may underestimate their role in the ecosystem maintenance.

DNA intercalating agents such as propidium monoazide (PMA) covalently bind with DNA molecules upon photolysis using visible light, and make it unavailable for DNA polymerase enzyme during polymerase chain reaction (PCR). Environmental DNA samples will be treated with suboptimum PMA concentration, enough to intercalate with 90–99% of the total DNA. The probability of PMA binding with DNA from abundant bacterial species will be much higher than binding with DNA from less abundant species. This will increase the relative DNA concentration of previously "shadowed" less abundant species available for PCR amplification. These PCR products obtained with and without PMA treatment will then be subjected to downstream diversity analyses such as sequencing and DNA microarray. It is expected that PMA-coupled PCR will amplify the "minority population" and help in understanding microbial diversity spectrum of an environmental sample at a much deeper level.

This new protocol aims to overcome the major potential biases faced when analyzing microbial 16S rRNA gene diversity. This study will lead to a technological advancement and a commercial product that will aid microbial ecologists in understanding microbial diversity from various environmental niches. Implementation of this technique may lead to discoveries of novel microbes and their functions in sustenance of the ecosystem.

This work was done by Parag A. Vaishampayan and Kasthuri J. Venkateswaran of Caltech for NASA's Jet Propulsion Laboratory. Further information is contained in a TSP (see page 1). NPO-48200

Laser Ablation Electrodynamic Ion Funnel for *In Situ* Mass Spectrometry on Mars

NASA's Jet Propulsion Laboratory, Pasadena, California

A front-end instrument, the laser ablation ion funnel, was developed, which would ionize rock and soil samples in the ambient Martian atmosphere, and efficiently transport the product ions into a mass spectrometer for *in situ* analysis.

Laser ablation creates elemental ions from a solid with a high-power pulse within ambient Mars atmospheric conditions. Ions are captured and focused with an ion funnel into a mass spectrometer for analysis. The electrodynamic ion fun-

nel consists of a series of axially concentric ring-shaped electrodes whose inside diameters (IDs) decrease over the length of the funnel. DC potentials are applied to each electrode, producing a smooth potential slope along the axial direction. Two radio-frequency (RF) AC potentials, equal in amplitude and 180° out of phase, are applied alternately to the ring electrodes. This creates an effective potential barrier along the inner surface of the electrode stack. Ions entering the

funnel drift axially under the influence of the DC potential while being restricted radially by the effective potential barrier created by the applied RF. The net result is to effectively focus the ions as they traverse the length of the funnel.

This work was done by Paul V. Johnson and Robert P. Hodyss of Caltech, and Keqi Tang and Richard D. Smith of PNNL for NASA's Jet Propulsion Laboratory. For more information, contact iaoffice@jpl.nasa.gov. NPO-47638

## High-Altitude MMIC Sounding Radiometer for the Global Hawk Unmanned Aerial Vehicle

This instrument can be used for improved weather forecasting and environmental monitoring.

NASA's Jet Propulsion Laboratory, Pasadena, California

Microwave imaging radiometers operating in the 50–183 GHz range for retrieving atmospheric temperature and water vapor profiles from airborne platforms have been limited in the spatial scales of atmospheric structures that are resolved not because of antenna aperture size, but because of high receiver noise masking the small variations that occur on small spatial scales. Atmospheric variability on short spatial and temporal scales (second/km scale) is completely unresolved by existing microwave profilers.

The solution was to integrate JPL-designed, high-frequency, low-noise-amplifier (LNA) technology into the High-Altitude MMIC Sounding Radiometer (HAMSR), which is an airborne microwave sounding radiometer, to lower the system noise by an order of magnitude to enable the instrument to resolve atmospheric variability on small spatial and temporal scales.

HAMSR has eight sounding channels near the 60-GHz oxygen line complex, ten channels near the 118.75-GHz oxygen line, and seven channels near the 183.31-GHz water vapor line. The HAMSR receiver system consists of three heterodyne spectrometers cover-
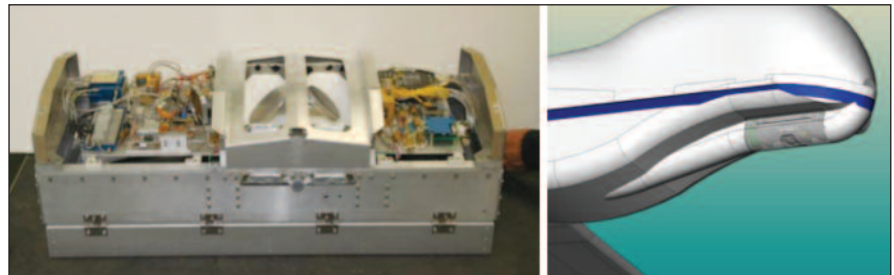
The **HAMSR Instrument** (left) is deployed in a forward bay under the nose of the **Global Hawk** aircraft (right).

ing the three bands. The antenna system consists of two back-to-back reflectors that rotate together at a programmable scan rate via a stepper motor. A single full rotation includes the swath below the aircraft followed by observations of ambient (roughly 0 °C in flight) and heated (70 °C) blackbody calibration targets located at the top of the rotation.

A field-programmable gate array (FPGA) is used to read the digitized radiometer counts and receive the reflector position from the scan motor encoder, which are then sent to a microprocessor and packed into data files. The microprocessor additionally

reads telemetry data from 40 onboard housekeeping channels (containing instrument temperatures), and receives packets from an onboard navigation unit, which provides GPS time and position as well as independent attitude information (e.g., heading, roll, pitch, and yaw). The raw data files are accessed through an Ethernet port. The HAMSR data rate is relatively low at 75 kbps, allowing for real-time access over the Global Hawk high-data-rate downlink. Once on the ground, the raw data are unpacked and processed through two levels of processing. The Level 1 product contains geo-located, time-stamped, calibrated brightness tempera-

tures for the Earth scan. These data are then input to a lD variational retrieval algorithm to produce temperature, water vapor, and cloud liquid water profiles, as well as several derived products such as potential temperature and relative humidity.

The addition of a state-of-the-art LNA to the 183-GHz receiver front-end and the upgrade of the 118-GHz LNA provide excellent low-noise performance, which is critical for microwave sounding retrievals. The data system is upgraded to provide in-flight data access through the Global Hawk data link, making it

possible to relay data to the ground in real time. This is particularly relevant for hurricane observations where HAMSR can provide real-time information on tropical storm structure, intensity, and evolution.

This instrument is the first to demonstrate the value of the technology through atmospheric water vapor measurements. The receiver noise was reduced by an order of magnitude compared to the previous receiver. A ground-based measurement campaign demonstrated unprecedented measurements of small-scale water vapor vari-

ability, resolving atmospheric fluctuations on meter and second space and time scales. Subsequent airborne measurements on the Global Hawk UAV showed similar results over a 40-km swath. This is a critical step in space-qualifying these receivers.

PRTs and Their Bonding for Long-Duration, Extreme-Temperature Environments

NASA's Jet Propulsion Laboratory, Pasadena, California

Research was conducted on the qualification of Honeywell platinum resistance thermometer (PRT) bonding for use in the Mars Science Laboratory (MSL). This is the first time these sensors will be used for Mars-related projects. Different types of PRTs were employed for the Mars Exploration Rover (MER) project, and several reliability issues were experienced, even for a short-duration mission like MER compared to MSL. Therefore, the development of a qualification process for the Honeywell PRT bonding was needed for the MSL project. Reliability of the PRT sensors,

and their bonding processes, is a key element to understand the health of the hardware during all stages of the project, and particularly during surface operations on Mars. Three extreme temperature summer season cycles and three winter season cycles (total: 1983 thermal cycles) were completed, and no Honeywell PRT failures associated with the bonding process were found.

Seventy-eight PRTs were bonded onto six different substrate materials using four different adhesives during the thermal cycling, which included a planetary protection cycle to +125 ºC

for two hours, three protoflight/qualification cycles (–135 to 70 ºC), 1,384 summer cycles (–105 to 40 ºC), and 599 winter cycles (–130 to 15 ºC). There were no observed changes in PRT resistances, bonding characteristics, or damage identified from the package evaluation as a result of the qualification tests.

Mid- and Long-IR Broadband Quantum Well Photodetector

NASA's Jet Propulsion Laboratory, Pasadena, California

A single-stack broadband quantum well infrared photodetector (QWIP) has been developed that consists of stacked layers of GaAs/AlGaAs quantum wells with absorption peaks centered at various wavelengths spanning across the 9-to-11-µm spectral regions. The correct design of broadband QWIPs was a critical step in this task because the earlier implementation of broadband QWIPs suffered from a tuning of spectral response curve with an applied bias. Here, a new QWIP design has been developed to overcome the spectral tuning with voltage that results from non-uniformity and bias variation of the electrical field

across the detector stacks with different absorption wavelengths.

In this design, a special effort has been made to avoid non-uniformity and bias tuning by changing the doping levels in detector stacks to compensate for variation of dark current generation rate across the stacks with different absorption wavelengths. Single-pixel photodetectors were grown, fabricated, and tested using this new design.

The measured dark current is comparable with the dark measured current for single-color QWIP detectors with similar cutoff wavelength, thus indicating high material quality as well as absence of per-

formance degradation resulting from broadband design. The measured spectra clearly demonstrate that the developed detectors cover the desired special range of 8 to 12 µm. Moreover, the shape of the spectral curves does not change with applied biases, thus overcoming the problem plaguing previous designs of broadband QWIPs.

3D Display Using Conjugated Multiband Bandpass Filters

NASA's Jet Propulsion Laboratory, Pasadena, California

Stereoscopic display techniques are based on the principle of displaying two views, with a slightly different perspective, in such a way that the left eye views only by the left eye, and the right eye views only by the right eye. However, one of the major challenges in optical devices is crosstalk between the two channels. Crosstalk is due to the optical devices not completely blocking the wrong-side image, so the left eye sees a little bit of the right image and the right eye sees a little bit of the left image. This results in eyestrain and headaches.

A pair of interference filters worn as an optical device can solve the problem. The device consists of a pair of multiband bandpass filters that are conjugated. The term "conjugated" describes the passband regions of one filter not overlapping with those of the other, but the regions are interdigitated. Along with the glasses, a 3D display produces colors composed of primary colors (basis for producing colors) having the spectral bands the same as the passbands of the filters. More specifically, the primary colors producing one viewpoint will be made

up of the passbands of one filter, and those of the other viewpoint will be made up of the passbands of the conjugated filter. Thus, the primary colors of one filter would be seen by the eye that has the matching multiband filter. The inherent characteristic of the interference filter will allow little or no transmission of the wrong side of the stereoscopic images.

This work was done by Youngsam Bae and Victor E. White of Caltech, and Kirill Shcheglov of SBC Global for NASA's Jet Propulsion Laboratory. Further information is contained in a TSP (see page 1). NPO-47578

Real-Time, Non-Intrusive Detection of Liquid Nitrogen in Liquid Oxygen at High Pressure and High Flow

Stennis Space Center, Mississippi

An integrated fiber-optic Raman sensor has been designed for real-time, non-intrusive detection of liquid nitrogen in liquid oxygen (LOX) at high pressures and high flow rates in order to monitor the quality of LOX used during rocket engine ground testing. The integrated sensor employs a high-power (3-W) Melles Griot diode-pumped, solid-state (DPSS), frequency-doubled Nd:YAG 532-nm laser; a modified Raman probe that has built-in Raman signal filter optics;

two high-resolution spectrometers; and photomultiplier tubes (PMTs) with selected bandpass filters to collect both N_2 and O_2 Raman signals.

The PMT detection units are interfaced with National Instruments' LabVIEW for fast data acquisition. Studies of sensor performance with different detection systems (i.e., spectrometer and PMT) were carried out. The concentration ratio of N_2 and O_2 can be inferred by comparing the intensities of the N_2

and O_2 Raman signals. The final system was fabricated to measure N_2 and O_2 gas mixtures as well as mixtures of liquid N_2 and LOX.

This work was done by Jagdish P. Singh and Fang-Yu Yueh of Mississippi State University, and Rajamohan R.Kalluru and Louie Harrison of Mississippi Ethanol LLC for Stennis Space Center. For more information contact Jagdish Singh at (662) 325-7375. Refer to SSC-00322.

Method to Enhance the Operation of an Optical Inspection Instrument Using Spatial Light Modulators

The interferometer would accommodate a large variety of spherical and aspherical optical components.

Goddard Space Flight Center, Greenbelt, Maryland

For many aspheric and freeform optical components, existing interferometric solutions require a custom computer-generated hologram (CGH) to characterize the part. The overall objective of this research is to develop hardware and a procedure to produce a combined, dynamic, Hartmann/Digital Holographic interferometry inspection system for a wide range of advanced optical components, including aspheric and freeform optics. This new in-

strument would have greater versatility and dynamic range than currently available measurement systems.

The method uses a spatial light modulator to pre-condition wavefronts for imaging, interferometry, and data processing to improve the resolution and versatility of an optical inspection instrument. Existing interferometers and Hartmann inspection systems have either too small a dynamic range or insuf-

ficient resolution to characterize conveniently unusual optical surfaces like aspherical and freeform optics. For interferometers, a specially produced, computer-generated holographic optical element is needed to transform the wavefront to within the range of the interferometer.

A new hybrid wavefront sensor employs newly available spatial light modulators (SLMs) as programmable holographic

optical elements (HOEs). The HOE is programmed to enable the same instrument to inspect an optical element in stages, first by a Hartmann measurement, which has a very large dynamic range but less resolution. The first measurement provides the information required to precondition a reference wave that avails the measurement process to the more precise phase shifting interferometry.

The SLM preconditions a wavefront before it is used to inspect an optical component. This adds important features to an optical inspection system, enabling not just wavefront conditioning for null testing and dynamic range extension, but also the creation of hybrid measurement procedures. This, for example, allows the combination of dynamic digital holography and Hartmann sensing procedures to cover a virtually unlimited dynamic range with high resolution. Digital holography technology brings all of the power and benefits of digital holographic interferometry to the requirement, while Hartmann-type wavefront sensors bring deflectometry technologies to the solution.

The SLM can be used to generate arbitrary wavefronts in one leg of the interferometer, thereby greatly simplifying its use and extending its range. The SLM can also be used to modify the system into a dynamic Shack-Hartmann system, which is useful for optical components with large amounts of slope. By integrating these capabilities into a single instrument, the system will have tremendous flexibility to measure a variety of optical shapes accurately.

Books & Reports

⚙ Dual-Compartment Inflatable Suitlock

A paper discusses a dual-compartment inflatable suitlock (DCIS) for Extravehicular Activity (EVA) that will allow for dust control, suit maintenance, and efficient EVA egress/ingress. The expandable (inflatable technologies) aspect of the design will allow the unit to stow in a compact package for transport.

The DCIS consists of three hard, inline bulkheads, separating two cylindrical membrane-walled compartments. The inner bulkhead can be fitted with a variety of hatch types, docking flanges, and mating hardware, such as the common berthing mechanism (CBM), for the purpose of mating with vehicles, habitats, and other pressurized modules. The inner bulkhead and center bulkhead function as the end walls of the inner compartment, which, during operations, would stay pressurized, either matching the pressure of the habitat or acting as a lower-pressure transitional volume. The suited crewmember can quickly don a suit, and egress the suitlock without waiting for the compartment to depressurize. The outer compartment can be pressurized infrequently, when a long dwell time is expected prior to the next EVA, or during off-nominal suit maintenance tasks, allowing "shirtsleeve" inspections and maintenance of the space suits. The outer bulkhead has a pressure-assisted hatch door that stays open and stowed routinely, but can be closed for suit maintenance and pressurization as needed.

This work was done by A. Scott Howe of Caltech, and Kriss J. Kennedy, Peggy L. Guirgis, and Robert M. Boyle of Johnson Space Center for NASA's Jet Propulsion Laboratory. Further information is contained in a TSP (see page 1). NPO-47786

⌷ Large-Strain Transparent Magnetoactive Polymer Nanocomposites

A document discusses polymer nanocomposite superparamagnetic actuators that were prepared by the addition of organically modified superparamagnetic nanoparticles to the polymer matrix. The nanocomposite films exhibited large deformations under a magnetostatic field with a low loading level of 0.1 wt% in a thermoplastic polyurethane elastomer (TPU) matrix. The maximum actuation deformation of the nanocomposite films increased exponentially with increasing nanoparticle concentration.

The cyclic deformation actuation of a high-loading magnetic nanocomposite film was examined in a low magnetic field, and it exhibited excellent reproducibility and controllability. Low-loading TPU nanocomposite films (0.1–2 wt%) were transparent to semi-transparent in the visible wavelength range, owing to good dispersion of the magnetic nanoparticles. Magnetoactuation phenomena were also demonstrated in a high-modulus, high-temperature polyimide resin with less mechanical deformation.

This work was done by Michael A. Meador of Glenn Research Center and Mitra Yoonessi of the Ohio Aerospace Institute. Further information is contained in a TSP (see page 1).

Inquiries concerning rights for the commercial use of this invention should be addressed to NASA Glenn Research Center, Innovative Partnerships Office, Attn: Steven Fedor, Mail Stop 4–8, 21000 Brookpark Road, Cleveland, Ohio 44135. Refer to LEW-18752-1.

◈ Thermodynamic Vent System for an On-Orbit Cryogenic Reaction Control Engine

A report discusses a cryogenic reaction control system (RCS) that integrates a Joule-Thompson (JT) device (expansion valve) and thermodynamic vent system (TVS) with a cryogenic distribution system to allow fine control of the propellant quality (subcooled liquid) during operation of the device. It enables zero-venting when coupled with an RCS engine. The proper attachment locations and sizing of the orifice are required with the propellant distribution line to facilitate line conditioning. During operations, system instrumentation was strategically installed along the distribution/TVS line assembly, and temperature control bands were identified.

A sub-scale run tank, full-scale distribution line, open-loop TVS, and a combination of procured and custom-fabricated cryogenic components were used in the cryogenic RCS build-up. Simulated on-orbit activation and thruster firing profiles were performed to quantify system heat gain and evaluate the TVS's capability to maintain the required propellant conditions at the inlet to the engine valves. Test data determined that a small control valve, such as a piezoelectric, is optimal to provide continuously the required thermal control. The data obtained from testing has also assisted with the development of fluid and thermal models of an RCS to refine integrated cryogenic propulsion system designs.

This system allows a liquid oxygen-based main propulsion and reaction control system for a spacecraft, which improves performance, safety, and cost over conventional hypergolic systems due to higher performance, use of non-toxic propellants, potential for integration with life support and power subsystems, and compatibility with *in-situ* produced propellants.

This work was done by Eric A. Hurlbert, Kris A. Romig, Rafael Jimenez, and Sam Flores of Johnson Space Center. Further information is contained in a TSP (see page 1). MSC-24543-1

⚙ Time Distribution Using SpaceWire in the SCaN Testbed on ISS

A paper describes an approach for timekeeping and time transfer among the devices on the CoNNeCT project's SCaN Testbed. It also describes how the clocks may be synchronized with an external time reference; e.g., time tags from the International Space Station (ISS) or RF signals received by a radio (TDRSS time service or GPS).

All the units have some sort of counter that is fed by an oscillator at some convenient frequency. The basic problem in timekeeping is relating the counter value to some external time standard such as UTC.

With SpaceWire, there are two approaches possible: one is to just use SpaceWire to send a message, and use an external wire for the sync signal. This is much the same as with the RS-232 messages and l pps line from a GPS receiver. However, SpaceWire has an additional capability that was added to make it easier — it can insert and receive a special "timecode" word in the data stream.

Another method is to use the SpaceWire time code features. A standard SpaceWire interface provides four signals: Tick In, Time In, Time Out, and Tick Out. When one end of the SpaceWire link asserts "Tick In," some small amount of time later (a few microseconds), Tick Out at the other end of the link is asserted. So there is a "virtual" wire connection over the SpaceWire link that can do synchronization (with an uncertainty and latency on the order of a few microseconds). The Time In signal provides an interface to send a 6-bit time code that is transparently inserted in the stream of data and control tokens being carried across the link, and recovered and presented on the Time Out at the destination without needing to create a special "time message."

This work was done by James P. Lux of Caltech for NASA's Jet Propulsion Laboratory. Further information is contained in a TSP (see page 1). NPO-47437

⊒ Techniques for Solution-Assisted Optical Contacting

A document discusses a "solution-assisted contacting" technique for optical contacting. An optic of surface flatness Lambda/20 was successfully contacted with one of "moderate" surface quality, or Lambda/4. Optics used were both ultra-low expansion (ULE) glass (Lambda/4 and Lambda/20) and fused silica (Lambda/20).
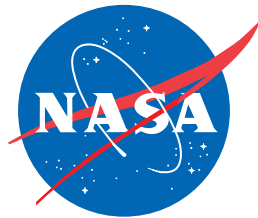
A stainless steel template of the intended interferometer layout was designed and constructed with three contact points per optic. The contact points were all on a common side of the template. The entire contacting jig was tilted at about 30°. Thus, when the isopropanol was applied, each optic slid due to gravity, resting on the contact points.

All of the contacting was performed in a relatively dusty laboratory. A number of successful contacts were achieved where up to two or three visible pieces of dust could be seen. These were clearly visible due to refraction patterns between the optic and bench. On a number of optics, the final step of dropping isopropyl between the surfaces was repeated until a successful contact was achieved.

The new procedures realized in this work represent a simplification for optical contacting in the laboratory. They will both save time and money spent during the contacting process, and research and development phases. The techniques outlined are suitable for laboratory experiments, research, and initial development stages.

This work was done by Glenn De Vine, Brent Ware, Danielle M. Wuchenich, Robert E. Spero, William M. Klipstein, and Kirk McKenzie of Caltech for NASA's Jet Propulsion Laboratory. Further information is contained in a TSP (see page 1). NPO-47963

National Aeronautics and
Space Administration